Scalable Spin Squeezing for Quantum-Enhanced Magnetometry with Bose-Einstein Condensates

W. Muessel,* H. Strobel, D. Linnemann, D. B. Hume, and M. K. Oberthaler
Kirchhoff-Institut für Physik, Universität Heidelberg, Im Neuenheimer Feld 227, 69120 Heidelberg, Germany
(Received 15 May 2014; published 5 September 2014)

A major challenge in quantum metrology is the generation of entangled states with a macroscopic atom number. Here, we demonstrate experimentally that atomic squeezing generated via nonlinear dynamics in Bose-Einstein condensates, combined with suitable trap geometries, allows scaling to large ensemble sizes. We achieve a suppression of fluctuations by 5.3(5) dB for 12 300 particles, from which we infer that similar squeezing can be obtained for more than 10^7 atoms. With this resource, we demonstrate quantum-enhanced magnetometry by swapping the squeezed state to magnetically sensitive hyperfine levels that have negligible nonlinearity. We find a quantum-enhanced single-shot sensitivity of 310(47) pT for static magnetic fields in a probe volume as small as 90 μm^3.

DOI: 10.1103/PhysRevLett.113.103004 PACS numbers: 37.25.+k, 03.75.Gg, 06.20.-f, 07.55.Ge

Atom interferometry [1] is a powerful technique for the precise measurement of quantities such as acceleration, rotation, and frequency [2–5]. Since state-of-the-art atom interferometers already operate at the classical limit for phase precision [6,7], given by the projection noise $\Delta\theta_{\mathrm{cl}} = 1/\sqrt{N}$ [8] for N detected particles, quantum entangled input states are a viable route for further improving the sensitivity of these devices.

One class of such states is spin squeezed states, which outperform the classical limit at a level given by the metrological spin squeezing parameter ξ_{R} with $\Delta\theta_{\mathrm{sq}} = \xi_{\mathrm{R}}\Delta\theta_{\mathrm{cl}}$ [9,10]. In the photonic case, quantum-enhanced interferometry with squeezed states is routinely employed in optical gravitational wave detectors [11]. For atoms, proof-of-principle experiments have shown that spin squeezed states can be generated in systems ranging from high-temperature vapors to ultracold Bose-Einstein condensates (BECs) [12–21], surpassing the classical limit in atom interferometry [14,22], atomic magnetometers [19], and atomic clocks [23,24].

BECs are particularly well suited for applications that require long interrogation times, high spatial resolution, or control of motional degrees of freedom, such as in measurements of acceleration and rotation, due to their high phase-space density. However, in these systems scaling of the squeezed states to large particle numbers is intrinsically limited by density dependent losses, e.g., due to molecule formation. Keeping these processes negligible implies that, for larger numbers, the volume has to be increased, which in turn limits the generation of squeezed states due to uncontrolled nonlinear multimode dynamics. Here, we show how this limitation can be overcome by realizing an array of many individual condensates with an optical lattice, increasing the local trap frequencies but keeping the density small.

In our experiment, we simultaneously prepare up to 30 independent BECs by superimposing a deep 1D optical lattice (period 5.5 μm) on a harmonic trap with a large aspect ratio, which provides transverse confinement [see Fig. 1(a)]. Each lattice site contains a condensate with $N = 300$ to 600 atoms in a localized spatial mode and the internal state $|a\rangle = |F, m_F\rangle = |1, 1\rangle$ of the lowest hyperfine manifold. Using a two-photon radio frequency and microwave transition, we apply phase and amplitude controlled coupling of the states $|a\rangle$ and $|b\rangle = |2, -1\rangle$, forming an effective two-level system. A magnetic bias field of 9.12 G brings the system near a Feshbach resonance, changing the interspecies interaction and leading to the nonlinearity necessary for squeezed state preparation. The nonlinear evolution is governed by the one-axis twisting Hamiltonian $\mathcal{H} = \chi\hat{J}_z^2$ [25], where the interaction strength is parametrized by χ, and $\hat{J}_z = (\hat{N}_b - \hat{N}_a)/2$ is the z component of the Schwinger pseudospin. As indicated in Fig. 1(a), the evolution of an initial coherent spin state under this Hamiltonian leads to an elongated squeezed state with reduced quantum uncertainty along one direction. Details about the experimental sequence, which includes a spin-echo pulse to reduce the influence of technical fluctuations during state preparation, can be found in the Supplemental Material [26].

In order to get access to the axis of minimal fluctuations, we rotate the state by an angle α around its mean spin direction. A projective measurement of the population imbalance $z = 2J_z/N = (N_b - N_a)/N$ is implemented by state-selective absorption imaging [see Fig. 1(a)]. The lower quantum uncertainty of the state translates into reduced fluctuations of z for repeated experiments, and is quantified using the number squeezing parameter $\xi_{\mathrm{N}}^2 = N\mathrm{Var}(z)$ [26].

High-resolution imaging of the individual lattice sites allows us to study ξ_{N}^2 for different system sizes by summing the populations of several sites [see Fig. 1(b)]. We develop a relative squeezing analysis that is insensitive to the

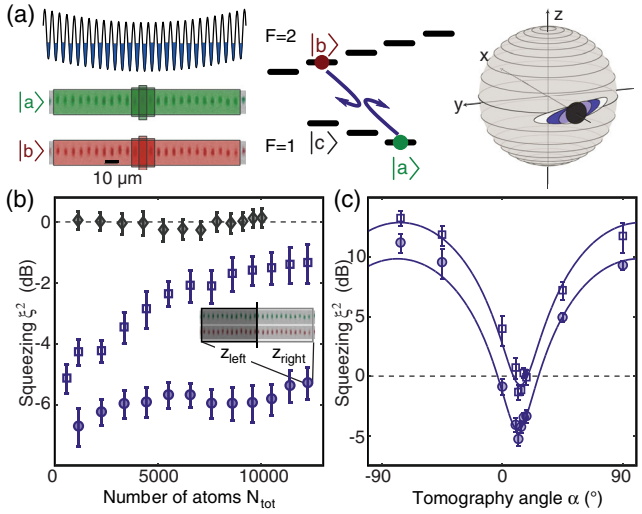

FIG. 1 (color online). Scaling squeezing to large ensemble sizes. (a) Independent squeezing (displayed on generalized Bloch sphere) of 25 binary BECs in a 1D lattice gives access to large atom numbers by summing over adjacent lattice sites. (b) Scaling of the squeezed state after 20 ms of nonlinear evolution. A relative analysis using adjacent parts of the lattice (inset) yields $\xi^2_{\mathrm{rel}} = -5.3(5)$ dB for the full sample of 12 300 atoms (blue circles), compared to $\xi^2_{\mathrm{N}} = -1.3(6)$ dB using direct analysis (open squares). The corresponding measurement for an initial coherent spin state (black diamonds) is at the classical shot noise limit. (c) Analysis for different tomography rotation angles α and 12 300 atoms shows the sinusoidal behavior from the redistributed uncertainties for direct (open squares) and relative analysis (filled circles). Error bars are the statistical 1 s.d. error.

magnetic field fluctuations present in our system (± 45 μG for several days). For that, we divide the lattice in half and evaluate the difference of the population imbalances $\delta z = z_{\mathrm{left}} - z_{\mathrm{right}}$ of the two regions [see inset Fig. 1(b)], which rejects common mode fluctuations. The corresponding squeezing parameter is given by $\xi^2_{\mathrm{rel}} = N_{\mathrm{tot}}\mathrm{Var}(\delta z)/4$ for equal particle numbers on both sides and $\langle z_i \rangle \approx 0$ [26], which is directly connected to the quantum enhancement of gradiometry as described below. We find $\xi^2_{\mathrm{rel}} = -5.3(5)$ dB for the full ensemble of 12 300 atoms after 20 ms of nonlinear evolution [Fig. 1(b), blue circles]. The remaining decrease of squeezing for large N_{tot} is due to the atom number dependent parameters of the single-site Hamiltonian. This affects the squeezing as well as the optimal tomography angles for different ensemble sizes. From our observations, we infer that by extending our one-dimensional array (30 lattice sites) to three dimensions (30^3 sites), ensembles as large as 10^7 atoms can be squeezed to the same level. Exploiting these resources does not require optically resolving the single lattice sites, and global population measurements are sufficient during the detection process.

To compare the scaling of our squeezed state with the best attainable classical state, we show the values of ξ^2_{rel} obtained for the initial coherent spin state (black diamonds), yielding the expected classical shot noise limit. In the case of squeezed states, even the direct analysis of summing all ensembles, which does not reject technical fluctuations, yields squeezing of $\xi^2_{\mathrm{N}} = -1.3(6)$ dB for 12 300 particles [Fig. 1(b), open blue squares]. For all given variances, the independently characterized photon shot noise of the detection process was subtracted.

Figure 1(c) shows the tomographic characterization of fluctuations for different readout rotation angles α for the ensemble containing 10^4 particles, revealing the expected sinusoidal behavior. The difference between the relative and the direct analysis is consistent with an independent characterization of the technical noise [26] and can be further reduced with an optimized spin-echo pulse.

A natural application of atomic squeezed states is the measurement of magnetic fields, where BECs are an ideal system to achieve both high sensitivity and spatial resolution [22,46,47]. We implement a quantum-enhanced magnetometer using a modified Ramsey sequence that coherently transfers the population of one level to a different hyperfine state for the interrogation time. The advantage of this state swapping is twofold: the nonlinear interaction becomes negligible on our interferometric time scales, and the magnetic sensitivity is significantly increased from ≈ 1 Hz/μT (second order Zeeman shift at the operating field of $B_0 = 9.12$ G) to $\mathcal{S} \approx 140$ Hz/μT (first order Zeeman shift). Figure 2(a) depicts the implemented experimental sequence. After generating the squeezed state in the levels $|a\rangle$ and $|b\rangle$ (left panel), we rotate it for maximum phase sensitivity (middle panel). The interrogation time t_{int} of the Ramsey sequence starts with a microwave π pulse (t_π) which swaps the level $|b\rangle$ of the phase squeezed state to the level $|c\rangle = |1,-1\rangle$, yielding increased magnetic sensitivity (right panel). After a hold time t_{hold}, we swap the state back to the original level. During this sequence, the state acquires a phase $\varphi = 2\pi[\mathcal{S}(B - B_0) + \delta](t_{\mathrm{hold}} + 2t_\pi)$, where δ describes the relative detuning of the π pulse. A Ramsey fringe is obtained by a final $\pi/2$ rotation with varied pulse phase ϕ.

First, we confirm that the level of squeezing is maintained during state swapping by performing an interferometric sequence with $t_{\mathrm{hold}} = 1$ μs followed by a tomographic analysis [Fig. 2(b)]. We find $\xi^2_{\mathrm{rel}} = -5.1^{+0.6}_{-0.7}$ dB at the optimum tomography angle and a Ramsey fringe visibility of $\mathcal{V} = 0.950(5)$ [Fig. 2(c)], revealing no significant reduction of the squeezing initially present. Without subtraction of detection noise, we find squeezing of $-3.8(5)$ dB, which corresponds to metrologically relevant spin squeezing of $-3.4(5)$ dB for the visibility $\mathcal{V} = 0.95$.

Since the single lattice sites are statistically independent, the single shot magnetic field sensitivity using this resource can be extracted from a differential measurement. This rejects common mode fluctuations of homogeneous fields,

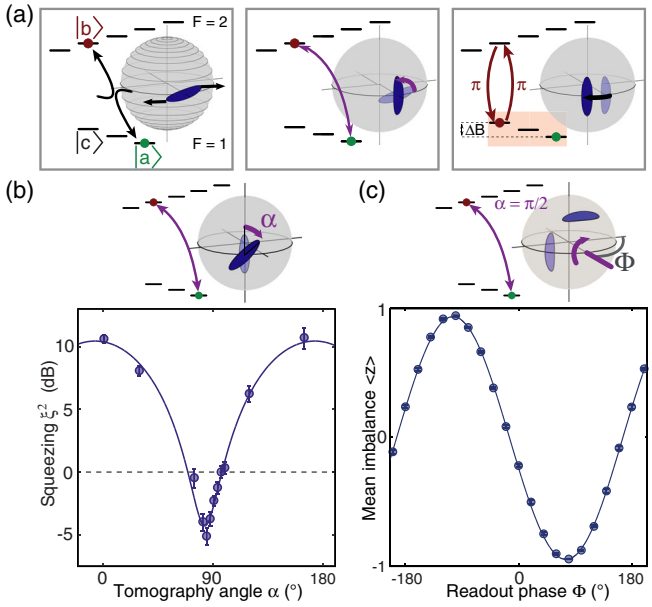

FIG. 2 (color online). Swapping squeezed states for a quantum-enhanced Ramsey scheme. (a) After 20 ms of nonlinear evolution on all lattice sites (left panel), the squeezed states are rotated to the phase sensitive axis (middle panel). By swapping the population from state $|b\rangle$ to $|c\rangle$, the nonlinearity is effectively switched off and the magnetic field sensitivity is significantly enhanced (right panel). After magnetic field-dependent phase evolution, the population is swapped back before readout. (b) Squeezing tomography after a hold time of 1 μs (negligible magnetic field phase) confirms relative squeezing of $\xi^2_{\mathrm{rel}} = -5.1^{+0.6}_{-0.7}$ dB [$-3.8(5)$ dB with detection noise] after swapping and readout. (c) Ramsey fringe for a final $\pi/2$ pulse with variable readout phase Φ yields a visibility of $\mathcal{V} = 0.950(5)$. This implies metrologically relevant spin squeezing of $-3.4(5)$ dB and direct applicability of the system for quantum-enhanced gradiometry. Error bars are the statistical 1 s.d. error.

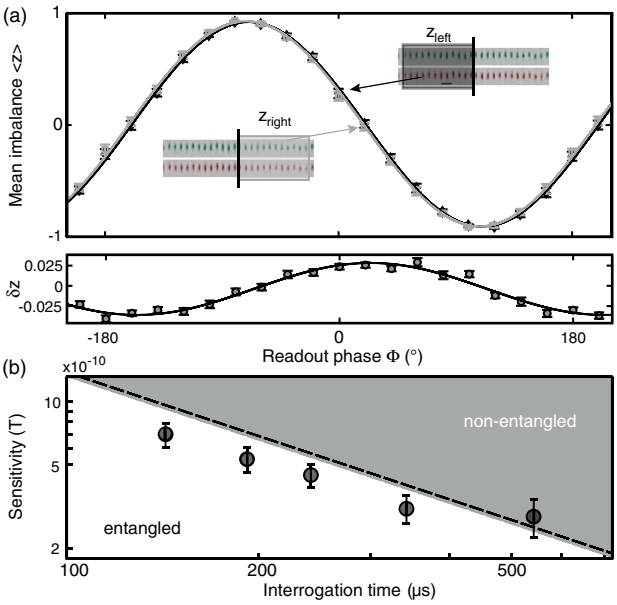

FIG. 3 (color online). Ramsey magnetometry beyond the standard quantum limit. (a) A magnetic field gradient translates into a phase shift of the corresponding Ramsey fringes for left and right parts of the full sample (upper panel for $t_{\mathrm{int}} = 342$ μs). The difference in population imbalance $\delta z = z_{\mathrm{left}} - z_{\mathrm{right}}$ is maximal at the zero crossings of the individual fringes (lower panel). (b) Magnetic field sensitivity of the Ramsey magnetometer versus interrogation time. For the full sample, we find quantum-enhanced performance up to interrogation times of 342 μs with a single shot sensitivity of 310(47) pT for static magnetic fields. For longer times, we are limited by fluctuations of the magnetic field. The shaded area depicts the region which is accessible for nonentangled states, the dashed line indicates the standard quantum limit including detection noise. Error bars show the statistical 1 s.d. confidence intervals obtained from a resampling method.

which would, otherwise, mask the actual sensitivity of the device. A magnetic field difference δB between the left and right part of the ensemble translates into a differential phase $\delta\varphi$ of the Ramsey fringes [Fig. 3(a)]. For a fixed pulse phase, this shows up as δz, the difference of the corresponding population imbalances. The optimal working point for estimating magnetic fields is close to the zero-crossings of the Ramsey fringes, where δz is maximal. At this point, the difference in the magnetic field can be deduced as $\delta B \approx (\delta z)_{\mathrm{max}}/2\pi t_{\mathrm{int}}\mathcal{S}\mathcal{V}$ with the interrogation time $t_{\mathrm{int}} = t_{\mathrm{hold}} + 2t_\pi$. The single shot magnetic field sensitivity around the optimal working point follows from error propagation in the expression for δB using the measured values for $\mathrm{Var}(\delta z)$ [26]. We find quantum-enhanced sensitivity up to interrogation times of 342 μs [see Fig. 3(b)]. For longer times, quantum enhancement is lost due to fluctuations of the magnetic field which translate into a significant reduction of the mean Ramsey contrast. We do not observe a decrease in single-shot visibility, indicating that no coherence is lost on these time scales.

For $t_{\mathrm{int}} = 342$ μs and the full ensemble, we find a quantum-enhanced single shot sensitivity for static magnetic fields of 310(47) pT compared to the shot noise limit of 382 pT for a perfect classical device (same atom number, no detection noise, and $\mathcal{V} = 1$). With our current experimental duty cycle (36 s production, 342 μs interrogation), we realized a sub–shot-noise sensitivity of $1.86(28)$ nT$/\sqrt{\mathrm{Hz}}$ for static magnetic fields. The performance of our magnetometer is competitive with state-of-the-art devices with comparably small probe volume [48], such as micro-superconducting quantum interference devices or nitrogen vacancy centers (see [26] for an overview). The ultimate physical limitation is the residual nonlinearity of the employed states, which implies that further improvement of the sensitivity by at least 2 orders of magnitude can be achieved by increasing the interrogation time. Thus, for an interrogation time of 250 ms [46] and assuming a realistic cycle time of 5 s for an all-optical BEC apparatus, a sensitivity of $\sim$1 pT$/\sqrt{\mathrm{Hz}}$ in a probe volume of just 90 μm^3 is feasible.

Our array of BECs is ideally suited for gradiometric measurements. The sensitivity for magnetic field gradients depends on interrogation time, the distance between the detectors (baseline length), and the noise of the magnetic field detection. We find the expected linear dependence of the signal amplitude $(\delta z)_{\max}$ on interrogation time, as shown in Fig. 4(a). The gradiometric sensitivity for the specific interrogation time of 342 μs as a function of baseline length is shown in Fig. 4(b). Using single wells with varying distances, we find the expected linear gain in gradient sensitivity with baseline length (triangles) and observe quantum enhancement beyond the respective classical limits (dashed line).

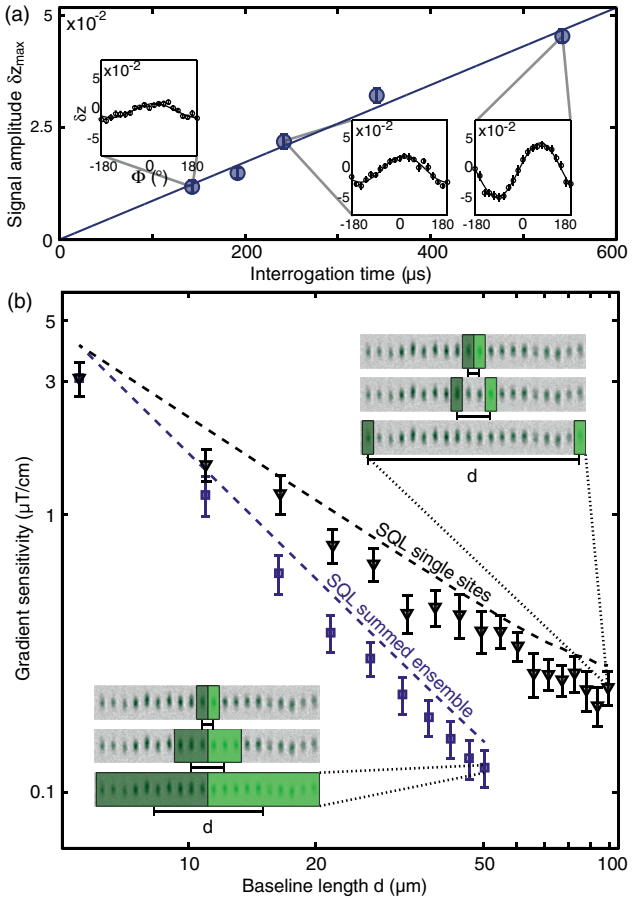

FIG. 4 (color online). Magnetic field gradiometry with an array of condensates. (a) A magnetic field gradient is deduced from the fringe amplitude of δz (insets), which grows linearly with interrogation time (blue circles and linear fit). We find $\partial B_z/\partial x = 19.6(6)$ pT/μm. (b) Gradiometric sensitivity for $t_{\rm int} = 342$ μs. For increasing baseline length d between single wells, we find a gain of gradient sensitivity (triangles) below the classical standard quantum limit (SQL, upper dashed line). The deviation from the expected linear behavior is due to the decrease of atom number toward the edges of the array. The sensitivity can be further increased (squares) by summing the populations of lattice sites as indicated in the inset, and beats the corresponding standard quantum limit for the summed ensemble (lower dashed line). Error bars are the 1 s.d. confidence from a resampling method.

The single shot sensitivity of the gradiometer can be further improved to 12(2) pT/μm by summing up to 20 adjacent lattice sites, exploiting the scalability of the squeezed state, and leading to an effective baseline length of up to 50 μm [Fig 4(b), squares]. This corresponds to a quantum-enhancement of 24%, as expected from the independently determined 2.4 dB of squeezing [see Fig. 2(b) at $\alpha = 90°$, here, without subtraction of detection noise]. Specifically for our experiment, we determine the magnetic field gradient to be $\partial B_z/\partial x = 19.6(6)$ pT/μm.

The high spatial resolution, combined with the excellent magnetic field sensitivity, makes the array of spin squeezed BECs an ideal system for magnetic field microscopy, where squeezing allows for enhanced sensitivity at small length scales. In contrast to atoms magnetically trapped on atom chips, optical confinement also allows vector field reconstruction with high spatial resolution.

In conclusion, we demonstrated the scalability of squeezed ensembles in an optical lattice, directly applicable to high-precision atom interferometry with ultracold clouds. We show that swapping of squeezed states is experimentally feasible and allows both for control of nonlinear interaction and the field sensitivity. Both advantages are explicitly demonstrated with quantum-enhanced Ramsey magnetometry, achieving high sensitivity and spatial resolution. The flexibility of state swapping with large squeezed ensembles offers prospects for improved tests of general relativity or the detection of gravitational waves with atom interferometers employing motional degrees of freedom [49,50], controlled by Raman beam splitters. From a more fundamental perspective, the system of several independent ensembles entangled in the internal degrees of freedom combined with adjustable tunnel coupling is a perfect starting point to study the spread of quantum correlations [51,52] in the continuous variable limit and the role of entanglement in quantum phase transitions [53,54].

We thank I. Stroescu and J. Schulz for technical help and discussions. This work was supported by the Heidelberg Center for Quantum Dynamics and the European Commission small or medium-scale focused research project QIBEC (Quantum Interferometry with Bose-Einstein condensates, Contract No. 284584). W. M. acknowledges support by the Studienstiftung des deutschen Volkes. D. B. H. acknowledges support from the Alexander von Humboldt foundation.

*ScalableSqueezing@matterwave.de

[1] A. D. Cronin, J. Schmiedmayer, and D. E. Pritchard, Rev. Mod. Phys. **81**, 1051 (2009).
[2] R. Geiger *et al.*, Nat. Commun. **2**, 474 (2011).

[3] A. Peters, K. Y. Cung, and S. Chu, Metrologia **38**, 25 (2001).
[4] T. L. Gustavson, P. Bouyer, and M. A. Kasevich, Phys. Rev. Lett. **78**, 2046 (1997).
[5] R. Wynands and S. Weyers, Metrologia **42**, S64 (2005).
[6] S. M. Dickerson, J. M. Hogan, A. Sugarbaker, D. M. S. Johnson, and M. A. Kasevich, Phys. Rev. Lett. **111**, 083001 (2013).
[7] D. S. Durfee, Y. K. Shaham, and M. A. Kasevich, Phys. Rev. Lett. **97**, 240801 (2006).
[8] W. M. Itano, J. C. Bergquist, J. J. Bollinger, J. M. Gilligan, D. J. Heinzen, F. L. Moore, M. G. Raizen, and D. J. Wineland, Phys. Rev. A **47**, 3554 (1993).
[9] D. J. Wineland, J. J. Bollinger, W. M. Itano, and D. J. Heinzen, Phys. Rev. A **50**, 67 (1994).
[10] V. Giovannetti, S. Lloyd, and L. Maccone, Science **306**, 1330 (2004).
[11] The LIGO Scientific Collaboration, Nat. Phys. **7**, 962 (2011).
[12] J. Estève, C. Gross, A. Weller, S. Giovanazzi, and M. K. Oberthaler, Nature (London) **455**, 1216 (2008).
[13] J. Appel, P. J. Windpassinger, D. Oblak, U. B. Hoff, N. Kjærgaard, and E. S. Polzik, Proc. Natl. Acad. Sci. U.S.A. **106**, 10960 (2009).
[14] C. Gross, T. Zibold, E. Nicklas, J. Estève, and M. K. Oberthaler, Nature (London) **464**, 1165 (2010).
[15] M. F. Riedel, P. Böhi, Y. Li, T. W. Hänsch, A. Sinatra, and P. Treutlein, Nature (London) **464**, 1170 (2010).
[16] I. D. Leroux, M. H. Schleier-Smith, and V. Vuletić, Phys. Rev. Lett. **104**, 073602 (2010).
[17] M. H. Schleier-Smith, I. D. Leroux, and V. Vuletić, Phys. Rev. Lett. **104**, 073604 (2010).
[18] Z. Chen, J. G. Bohnet, S. R. Sankar, J. Dai, and J. K. Thompson, Phys. Rev. Lett. **106**, 133601 (2011).
[19] R. J. Sewell, M. Koschorreck, M. Napolitano, B. Dubost, N. Behbood, and M. W. Mitchell, Phys. Rev. Lett. **109**, 253605 (2012).
[20] T. Berrada, S. van Frank, R. Bücker, T. Schumm, J.-F. Schaff, and J. Schmiedmayer, Nat. Commun. **4**, 2077 (2013).
[21] J. G. Bohnet, K. C. Cox, M. A. Norcia, J. M. Weiner, Z. Chen, and J. K. Thompson, arXiv:1310.3177.
[22] C. F. Ockeloen, R. Schmied, M. F. Riedel, and P. Treutlein, Phys. Rev. Lett. **111**, 143001 (2013).
[23] A. Louchet-Chauvet, J. Appel, J. J. Renema, D. Oblak, N. Kjaergaard, and E. S. Polzik, New J. Phys. **12**, 065032 (2010).
[24] I. D. Leroux, M. H. Schleier-Smith, and V. Vuletić, Phys. Rev. Lett. **104**, 250801 (2010).
[25] M. Kitagawa and M. Ueda, Phys. Rev. A **47**, 5138 (1993).
[26] See Supplemental Material at http://link.aps.org/supplemental/10.1103/PhysRevLett.113.103004 for further comparison with other magnetometry techniques, details on the experimental sequence, and analysis methods, which includes Refs. [27–45].
[27] J. R. Maze *et al.*, Nature (London) **455**, 644 (2008).
[28] G. Balasubramanian *et al.*, Nat. Mater. **8**, 383 (2009).
[29] S. Steinert, F. Dolde, P. Neumann, A. Aird, B. Naydenov, G. Balasubramanian, F. Jelezko, and J. Wrachtrup, Rev. Sci. Instrum. **81**, 043705 (2010).
[30] V. M. Acosta, E. Bauch, A. Jarmola, L. J. Zipp, M. P. Ledbetter, and D. Budker, Appl. Phys. Lett. **97**, 174104 (2010).
[31] L. M. Pham, N. Bar-Gill, C. Belthangady, D. Le Sage, P. Cappellaro, M. D. Lukin, A. Yacoby, and R. L. Walsworth, Phys. Rev. B **86**, 045214 (2012).
[32] K. Jensen, N. Leefer, A. Jarmola, Y. Dumeige, V. M. Acosta, P. Kehayias, B. Patton, and D. Budker, Phys. Rev. Lett. **112**, 160802 (2014).
[33] A. Sandhu, A. Okamoto, I. Shibasaki, and A. Oral, Microelectron. Eng. **73–74**, 524 (2004).
[34] V. Shah, S. Knappe, P. D. Schwindt, and J. Kitching, Nat. Photonics **1**, 649 (2007).
[35] M. L. Terraciano, M. Bashkansky, and F. K. Fatemi, Phys. Rev. A **77**, 063417 (2008).
[36] H. B. Dang, A. C. Maloof, and M. V. Romalis, Appl. Phys. Lett. **97**, 151110 (2010).
[37] J. R. Kirtley, M. B. Ketchen, K. G. Stawiasz, J. Z. Sun, W. J. Gallagher, S. H. Blanton, and S. J. Wind, Appl. Phys. Lett. **66**, 1138 (1995).
[38] F. Baudenbacher, L. E. Fong, J. R. Holzer, and M. Radparvar, Appl. Phys. Lett. **82**, 3487 (2003).
[39] M. I. Faley, U. Poppe, K. Urban, D. N. Paulson, and R. L. Fagaly, J. Phys. Conf. Ser. **43**, 1199 (2006).
[40] W. Wildermuth, S. Hofferberth, I. Lesanovsky, S. Groth, P. Krüger, J. Schmiedmayer, and I. Bar-Joseph, Appl. Phys. Lett. **88**, 264103 (2006).
[41] Y. Eto, H. Ikeda, H. Suzuki, S. Hasegawa, Y. Tomiyama, S. Sekine, M. Sadgrove, and T. Hirano, Phys. Rev. A **88**, 031602(R) (2013).
[42] H. J. Mamin, T. H. Oosterkamp, M. Poggio, C. L. Degen, C. T. Rettner, and D. Rugar, Nano Lett. **9**, 3020 (2009).
[43] M. Koschorreck, M. Napolitano, B. Dubost, and M. W. Mitchell, Appl. Phys. Lett. **98**, 074101 (2011).
[44] W. Muessel, H. Strobel, M. Joos, E. Nicklas, I. Stroescu, J. Tomkovič, D. B. Hume, and M. K. Oberthaler, Appl. Phys. B **113**, 69 (2013).
[45] R. G. Miller, Biometrika **61**, 1 (1974).
[46] M. Vengalattore, J. M. Higbie, S. R. Leslie, J. Guzman, L. E. Sadler, and D. M. Stamper-Kurn, Phys. Rev. Lett. **98**, 200801 (2007).
[47] S. Aigner, L. Della Pietra, Y. Japha, O. Entin-Wohlman, T. David, R. Salem, R. Folman, and J. Schmiedmayer, Science **319**, 1226 (2008).
[48] D. Budker and D. F. J. Kimball, *Optical Magnetometry* (Cambridge University, Cambridge, England, 2013).
[49] P. W. Graham, J. M. Hogan, M. A. Kasevich, and S. Rajendran, Phys. Rev. Lett. **110**, 171102 (2013).
[50] S. Dimopoulos, P. W. Graham, J. M. Hogan, and M. A. Kasevich, Phys. Rev. Lett. **98**, 111102 (2007).
[51] M. Cheneau, P. Barmettler, D. Poletti, M. Endres, P. Schauß, T. Fukuhara, C. Gross, I. Bloch, C. Kollath, and S. Kuhr, Nature (London) **481**, 484 (2012).
[52] T. Langen, R. Geiger, M. Kuhnert, B. Rauer, and J. Schmiedmayer, Nat. Phys. **9**, 640 (2013).
[53] A. Osterloh, L. Amico, G. Falci, and R. Fazio, Nature (London) **416**, 608 (2002).
[54] T. J. Osborne and M. A. Nielsen, Phys. Rev. A **66**, 032110 (2002).